

ARTICLE



Targeting histone demethylase LSD1 for treatment of deficits in autism mouse models

Maximiliano Rapanelli¹, Jamal B. Williams¹, Kaijie Ma¹, Fengwei Yang¹, Ping Zhong¹, Rajvi Patel¹, Manasa Kumar¹, Luye Qin¹, Benjamin Rein¹, Zi-Jun Wang¹, Bibi Kassim², Behnam Javidfar², Lizette Couto², Schahram Akbarian^{1,2} and Zhen Yan¹✉

© The Author(s), under exclusive licence to Springer Nature Limited 2022

Large-scale genetic studies have revealed that the most prominent genes disrupted in autism are chromatin regulators mediating histone methylation/demethylation, suggesting the central role of epigenetic dysfunction in this disorder. Here, we show that histone lysine 4 dimethylation (H3K4me2), a histone mark linked to gene activation, is significantly decreased in the prefrontal cortex (PFC) of autistic human patients and mutant mice with the deficiency of top-ranking autism risk factor *Shank3* or *Cul3*. A brief treatment of the autism models with highly potent and selective inhibitors of the H3K4me2 demethylase LSD1 (KDM1A) leads to the robust rescue of core symptoms of autism, including social deficits and repetitive behaviors. Concomitantly, LSD1 inhibition restores NMDA receptor function in PFC and AMPA receptor-mediated currents in striatum of *Shank3*-deficient mice. Genome-wide RNAseq and ChIPseq reveal that treatment of *Shank3*-deficient mice with the LSD1 inhibitor restores the expression and H3K4me2 occupancy of downregulated genes enriched in synaptic signaling and developmental processes. The immediate early gene tightly linked to neuronal plasticity, *Egr1*, is on the top list of rescued genes. The diminished transcription of *Egr1* is recapitulated in PFC of autistic human patients. Overexpression of *Egr1* in PFC of *Shank3*-deficient mice ameliorates social preference deficits. These results have for the first time revealed an important role of H3K4me2 abnormality in ASD pathophysiology, and the therapeutic potential of targeting H3K4me2 demethylase LSD1 or the downstream molecule *Egr1* for ASD.

Molecular Psychiatry; <https://doi.org/10.1038/s41380-022-01508-8>

INTRODUCTION

Autism spectrum disorder (ASD) is a complex and prevalent neurodevelopmental disease characterized by social impairments and repetitive behaviors. Genetic studies have revealed that aberrations in epigenetic modifiers that produce lysine methylation/demethylation to histones are the most prominent risk factors in ASD and other neurodevelopmental disorders (NDD) [1–4]. The balance between histone methyltransferases and demethylases is a tightly orchestrated process during normal development [5]. Mutations in histone demethylases, such as LSD1 (KDM1A), KDM3A, KDM4B, KDM5B, KDM6A, and KDM6B, and histone methyltransferases, including KMT2C (MLL3), ASH1L, SETD5, and SETD1A, have been identified in ASD or NDD [1, 2, 6]. These mutations that lead to imbalance of histone methylation/demethylation can have a deep impact on epigenetic regulation of gene expression, resulting in clinical symptoms of ASD and NDD [7]. Consistently, alterations in trimethylated H3K4 landscapes were found in the postmortem prefrontal cortex (PFC) of ASD patients [8].

To understand molecular mechanisms underlying the involvement of histone demethylases in autism, we mainly used *Shank3*-deficient mice in this study, because *SHANK3* haploinsufficiency is a highly penetrant causal factor for ASD and intellectual disabilities [9, 10]. *Shank3* is a scaffold protein in the postsynaptic density of glutamatergic synapses. Autistic behavioral deficits, including social deficits and stereotypic grooming, are manifested

in various *Shank3* mutant mouse lines [11–14]. Synaptic dysfunction and connectivity abnormality in the cortex and subcortical regions of these *Shank3*-deficient mice are thought to be the physiological basis of behavioral phenotypes [11–13, 15, 16].

In PFC of *Shank3*-deficient mice, the epigenetic enzymes that are linked to gene repression, histone deacetylase 2 (HDAC2) and H3K9 methyltransferases EHMT1/2, are upregulated, leading to gene downregulation, NMDAR hypofunction, and social deficits [11, 17]. An important component in HDAC/EHMT-containing chromatin-associated complex is the histone demethylase LSD1 [18–20]. LSD1 is responsible for demethylation of mono- and dimethylated lysine 4 of histone H3 (H3K4me and H3K4me2), which results in the loss of permissive histone marks and ensuing gene suppression. In this study, we focused on the functional role of transcriptional corepressor LSD1 and the therapeutic potential of targeting LSD1 in autism.

RESULTS

Autism patients and *Shank3*-deficient mice exhibit the significant loss of permissive H3K4me2 in PFC, which is reversed by inhibiting LSD1

To reveal the role of histone methylation in autism pathophysiology, we examined the global histone methylation that links to transcriptional activation, H3K4me2, in PFC, a key brain region

¹Department of Physiology and Biophysics, Jacobs School of Medicine and Biomedical Sciences, State University of New York at Buffalo, Buffalo, NY, USA. ²Department of Psychiatry; Friedman Brain Institute, Icahn School of Medicine at Mount Sinai, New York, NY, USA. ✉email: zhenyan@buffalo.edu

Received: 6 May 2021 Revised: 16 February 2022 Accepted: 23 February 2022

Published online: 16 March 2022

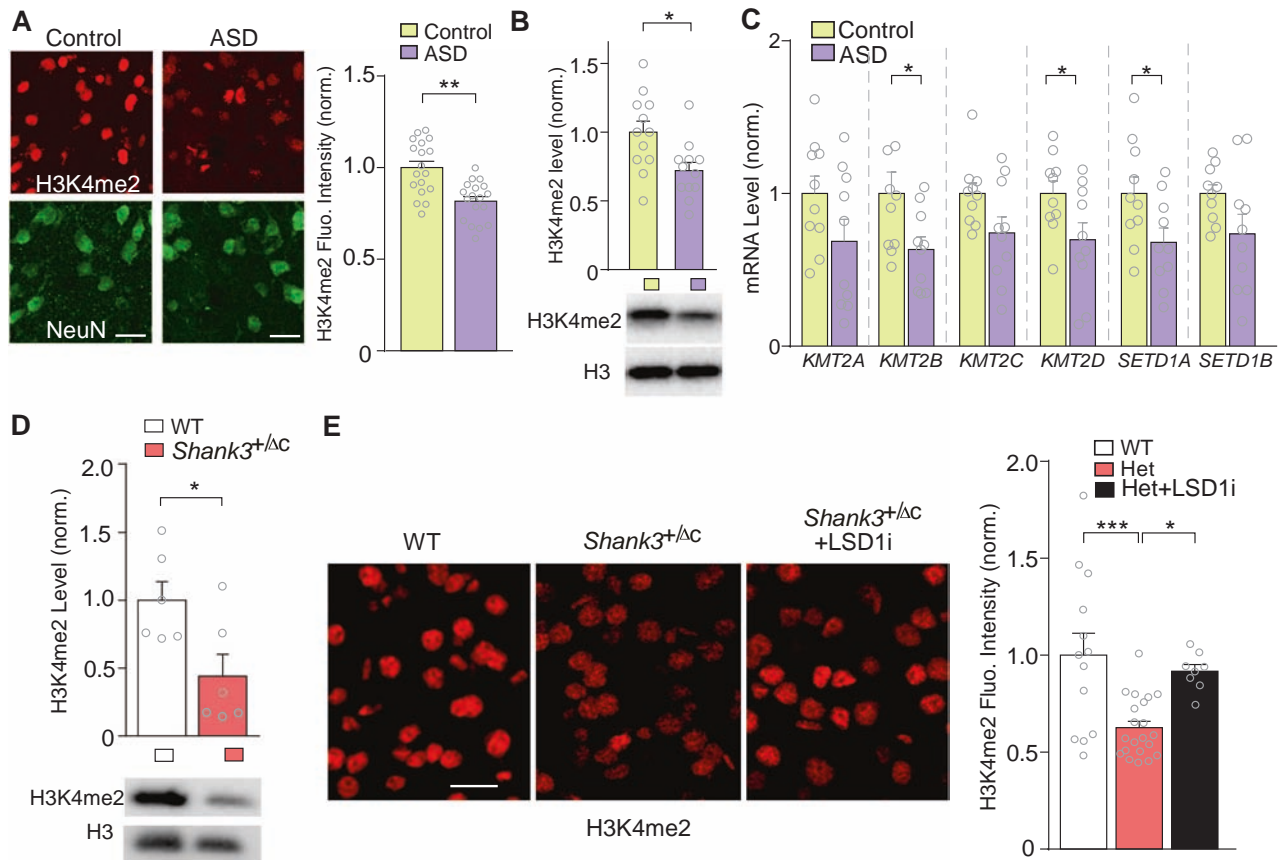


Fig. 1 Autistic patients and *Shank3*-deficient mice have diminished H3K4 dimethylation in PFC neurons, which is reversed by histone demethylase 1 (LSD1) inhibition. **A** Confocal images of immunohistochemical staining of H3K4me2 and NeuN in postmortem PFC tissues (BA9) from autism human patients (ASD) and control subjects. Scale bar: 20 μ m. Inset: Quantification of H3K4me2 (normalized to NeuN) in control ($n = 18$ slices/6 subjects) and ASD ($n = 18$ slices/6 subjects) humans ($t_{17} = 3.9$, $p = 0.001$, t -test). **B** Quantification of immunoblots of H3K4me2 (normalized to H3) in the nuclear fraction of PFC from ASD ($n = 12$) and control ($n = 12$) humans ($t_{22} = 2.77$, $p < 0.05$, t -test). Inset: representative blots of H3K4me2 and H3. **C** Bar graphs showing the mRNA level of H3K4me2-catalyzing enzymes *KMT2A/B/C/D* and *SETD1A/B* in PFC of ASD and control subjects ($n = 10$ subjects/group, *KMT2B*, $t_{18} = 2.24$, $p = 0.038$; *KMT2D*, $t_{18} = 2.18$, $p = 0.043$; *SETD1A*, $t_{18} = 2.23$, $p = 0.039$, t -test). **D** Quantification of immunoblots of H3K4me2 (normalized to H3) in the nuclear fraction of PFC from WT ($n = 5$) and *Shank3*^{+/-} ($n = 4$) mice ($t_{10} = 2.64$, $p = 0.025$, t -test). Inset: representative blots of H3K4me2 and H3. **E** Confocal images of H3K4me2 staining in PFC of WT vs. *Shank3*^{+/-} mice without or with the treatment of the LSD1 inhibitor GSK-LSD1 (LSD1i, 5 mg/kg, i.p., once daily for 3 days). Scale bar: 20 μ m. Inset: Quantification of H3K4me2 in the 3 groups (WT: $n = 13$ slices/7 mice, *Shank3*^{+/-}: $n = 21$ slices/7 mice, *Shank3*^{+/-} + LSD1i: $n = 8$ slices/4 mice, $F_{(2,39)} = 9.8$, $p = 0.0004$, one-way ANOVA). All data are mean \pm SEM. In all figures, * $p < 0.05$, ** $p < 0.01$, *** $p < 0.001$.

impaired in autism [21, 22]. Postmortem PFC tissues (Brodmann's area 9) from autism human patients vs. age and sex-matched control subjects (Supplementary Table 1) were first compared. Immunostaining of H3K4me2 indicated that PFC neurons (NeuN +) exhibited the significantly decreased H3K4me2 signaling in ASD patients, compared to control subjects (Fig. 1A). Immunoblotting confirmed the significantly decreased H3K4me2 level in PFC of ASD patients (Fig. 1B). Quantitative PCR profiling of histone modifying enzymes that catalyze H3K4me2 revealed that the mRNA level of *KMT2B*, *KMT2D*, and *SETD1A* was significantly lower in PFC of ASD patients (Fig. 1C), which could underlie the diminished H3K4me2 in autistic samples.

Immunoblotting also revealed the significantly reduced H3K4me2 level in PFC of *Shank3*^{+/-} mice (Fig. 1D). In contrast, no significant change was found in hippocampus and striatum of *Shank3*^{+/-} mice (Supplementary Fig. S1A, B), suggesting region specificity of this epigenetic change.

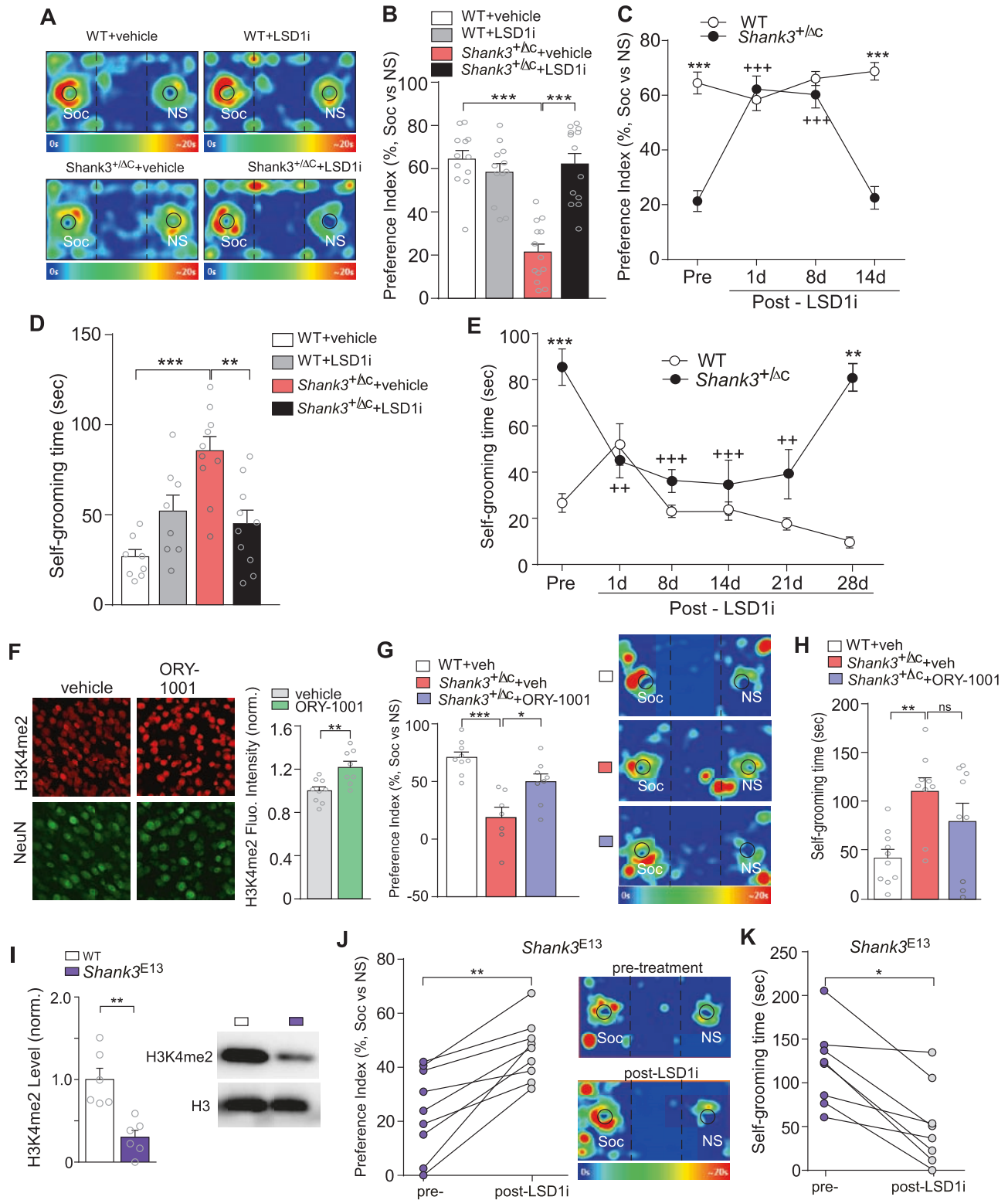
H3K4me2 is demethylated by lysine-specific histone demethylase 1 (LSD1, KDM1A). To normalize the diminished H3K4me2, we tested the effect of LSD1 inhibition in PFC of *Shank3*^{+/-} mice. GSK-LSD1 is a highly potent and selective LSD1 inhibitor with IC_{50} of 16 nM and >1000 fold selectivity over other closely related enzymes. Based on

the in vivo dose of GSK-LSD1 used in other treatment [23], we gave *Shank3*^{+/-} mice a systemic administration of GSK-LSD1 (5 mg/kg, i.p., once daily for 3 days). As shown in Fig. 1E, compared to WT mice, PFC neurons from *Shank3*^{+/-} mice had the significantly decreased H3K4me2 fluorescent intensity, similar to autistic human cases, and GSK-LSD1 treatment elevated H3K4me2 signaling to the control level. We also performed immunoblotting experiments to examine the effect of GSK-LSD1 at various time points. As shown in Supplementary Fig. S1C, D, GSK-LSD1 (5 mg/kg, i.p., 3x) induced a significant increase of H3K4me2 level in PFC on day 1, but not day 8 or day 14, after the cessation of treatment. This transient increase may provide a trigger to induce gene transcriptional changes.

Taken together, these data suggest that ASD patients and *Shank3*-deficient mice have abnormally low level of permissive H3K4me2 in PFC neurons, which can be normalized by treatment with the LSD1 inhibitor GSK-LSD1.

LSD1 inhibitors ameliorate social deficits and repetitive behaviors in autism models

Given the diminished H3K4me2 in *Shank3*^{+/-} mice, we next used the 3-chamber social preference assay to examine whether the autism-like social preference deficits in young male *Shank3*^{+/-}



mice [11, 12, 17, 24] could be rescued by specific inhibition of the H3K4me2 demethylase LSD1. A brief treatment of Shank3^{+/-ΔC} mice (5–6 weeks old) with GSK-LSD1 (5 mg/kg, i.p., 3x) significantly increased the time interacting with the social (Soc) stimulus over the time on nonsocial (NS) object (Fig. 2A). Compared to WT mice, the social preference index, $(T_{Soc} - T_{NS}) / (T_{Soc} + T_{NS})$, was profoundly diminished in Shank3^{+/-ΔC} mice, and was significantly elevated by GSK-LSD1 treatment (Fig. 2B). The therapeutic effect

of a single round of GSK-LSD1 treatment on social preference deficits in Shank3^{+/-ΔC} mice lasted for ~8 days post-injection (Fig. 2C).

Another core symptom of autism is repetitive behavior. As shown in Fig. 2D, Shank3^{+/-ΔC} mice spent significantly more time engaged in self-grooming, and GSK-LSD1 treatment dramatically reduced this repetitive behavior. Moreover, the therapeutic effect of a single round of GSK-LSD1 treatment on repetitive self-

Fig. 2 Treatment with LSD1 inhibitors rescues autism-like social deficits and repetitive behaviors in *Shank3*-deficient mice. **A** Representative heat maps illustrating the time spent investigating either the social (Soc) or nonsocial (NS) stimulus from the social preference tests of juvenile male WT and *Shank3*^{+/ Δ C} mice treated with GSK-LSD1 (LSD1i, 5 mg/kg, i.p., once daily for 3 days) or vehicle. **B** Bar graphs showing the preference index of the sociability testing in WT or *Shank3*^{+/ Δ C} mice treated with GSK-LSD1 or vehicle ($n = 12$ –13/group, $F_{(1,46)} = 31.4$, $p = 0.0001$; two-way ANOVA). **C** Plots of social preference index in WT or *Shank3*^{+/ Δ C} mice before and multiple days after treatment with GSK-LSD1 (WT: $n = 12$, *Shank3*^{+/ Δ C}: $n = 13$, $F_{(3,69)} = 30.7$, $p < 0.0001$; two-way repeated measure ANOVA). **D** Bar graphs showing the time spent on repetitive self-grooming in WT or *Shank3*^{+/ Δ C} mice treated with GSK-LSD1 or vehicle ($n = 8$ –10/group, $F_{(1,32)} = 19.1$, $p = 0.0001$; two-way ANOVA). **E** Plots of self-grooming time in WT or *Shank3*^{+/ Δ C} mice before and multiple (1, 8, 14, 21, 28) days after treatment with GSK-LSD1 (WT: $n = 8$, *Shank3*^{+/ Δ C}: $n = 10$; two-way repeated measure ANOVA). **F** Confocal images and quantification of H3K4me2 and NeuN staining in PFC of mice treated with ORY-1001 (0.015 mg/kg, i.p., 3x) or vehicle (veh: $n = 9$ slices/3 mice; ORY: $n = 8$ slices/3 mice, $t_{15} = 3.3$, $p = 0.005$, t -test). Scale bar: 20 μ m. **G** Bar graphs showing social preference index of WT or *Shank3*^{+/ Δ C} mice treated with ORY-1001 or vehicle ($n = 7$ –9/group, $F_{(2,21)} = 15.1$, $p < 0.001$, one-way ANOVA). Inset: Representative heat maps of the 3-chamber social preference test. **H** Bar graphs showing the time spent on repetitive self-grooming in WT or *Shank3*^{+/ Δ C} mice treated with ORY-1001 or vehicle ($n = 9$ –10/group, $F_{(2,25)} = 6.0$, $p < 0.01$, one-way ANOVA). **I** Quantification of immunoblots of H3K4me2 (normalized to H3) in the nuclear fraction of PFC from WT ($n = 6$) and *Shank3*^{E13} ($n = 6$) mice ($t_8 = 4.3$, $p = 0.023$, t -test). Inset: representative blots of H3K4me2 and H3. **J** Plot of social preference index in individual *Shank3*^{E13} mouse ($n = 9$) before and after GSK-LSD1 treatment ($t_{16} = 3.5$, $p = 0.003$, paired t -test). **K** Plot of time on self-grooming in individual *Shank3*^{E13} mouse ($n = 8$) before and after GSK-LSD1 treatment ($t_{14} = 2.9$, $p = 0.01$, paired t -test). All data are mean \pm SEM. In all figures, * $p < 0.05$, ** $p < 0.01$, *** $p < 0.0001$, WT vs. *Shank3*-deficient mice; ++ $p < 0.01$, +++ $p < 0.0001$, pre- vs. post-treatment.

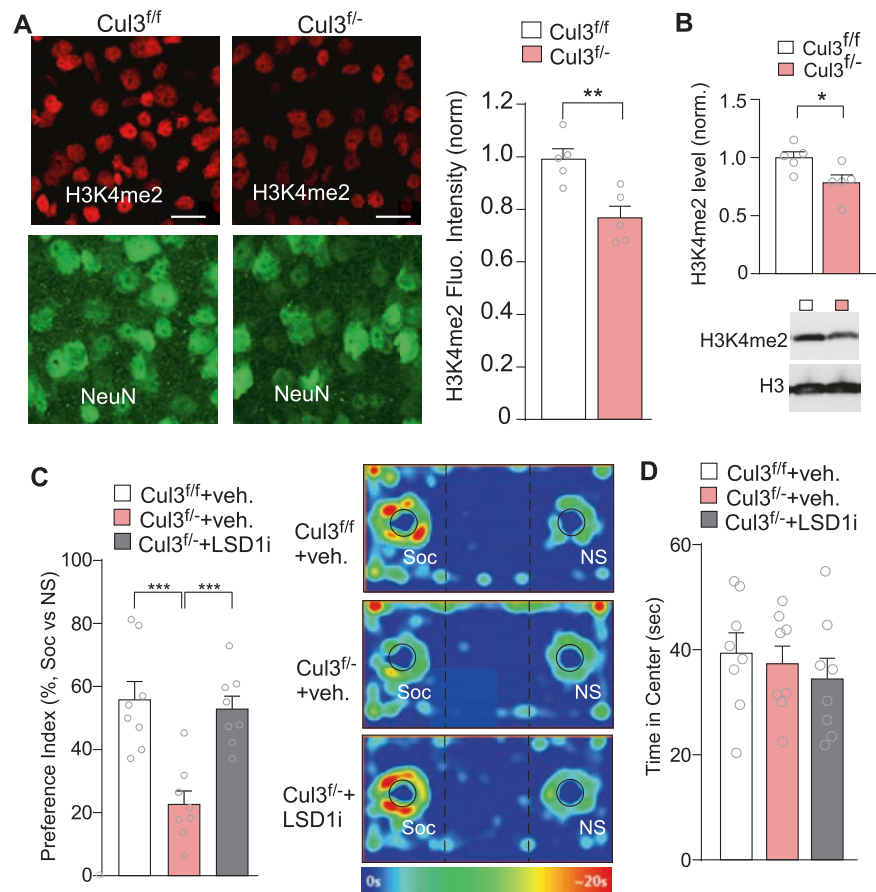


Fig. 3 Treatment with LSD1 inhibitor rescues social deficits in *Cul3* model of autism. **A** Confocal images of immunohistochemical staining of H3K4me2 and NeuN in PFC from heterozygous forebrain *Cul3* knockout mice (*Cul3*^{fl-/-}) and control (*Cul3*^{fl/fl}) mice. Scale bar: 20 μ m. Inset: Quantification of H3K4me2 (normalized to NeuN) in *Cul3*^{fl/fl} ($n = 15$ slices/5 mice) and *Cul3*^{fl-/-} ($n = 15$ slices/5 mice) ($t_8 = 3.7$, $p = 0.006$, t -test). **B** Bar graphs and representative blots showing the level of H3K4me2 (normalized to H3) in PFC of *Cul3*^{fl/fl} vs. *Cul3*^{fl-/-} mice ($n = 5$ mice per group, $t_8 = 2.53$, $p = 0.03$, t -test). **C** Bar graphs showing the social preference index of *Cul3*^{fl/fl} or *Cul3*^{fl-/-} mice treated with GSK-LSD1 (LSD1i, 5 mg/kg, i.p., 3x) or vehicle ($n = 8$ per group, $F_{(2,21)} = 14.6$, $p < 0.001$, one-way ANOVA). Inset: Representative heat maps of the 3-chamber sociability test. **D** Bar graphs showing the time in center in open-field tests of *Cul3*^{fl/fl} or *Cul3*^{fl-/-} mice treated with GSK-LSD1 or vehicle ($n = 8$ per group). All data are mean \pm SEM. In all figures, ** $p < 0.01$, *** $p < 0.001$.

grooming in *Shank3*^{+/ Δ C} mice sustained for ~21 days post-injection and disappeared at 28 days after treatment (Fig. 2E).

GSK-LSD1 treatment did not affect motor coordination as measured by rotarod tests (Supplementary Fig. S2A), general movement as measured by locomotor activity (Supplementary Fig. S2B) or anxiety level as measured by open-field tests

(Supplementary Fig. S2C). Blood chemistry and hematological analyses of GSK-LSD1-treated animals found that all the indicators for liver and kidney functions, as well as lipid and protein metabolism, were within normal ranges (Supplementary Table 2). These results indicate that GSK-LSD1 can lead to robust rescue of two primary phenotypes of autism, social deficits and

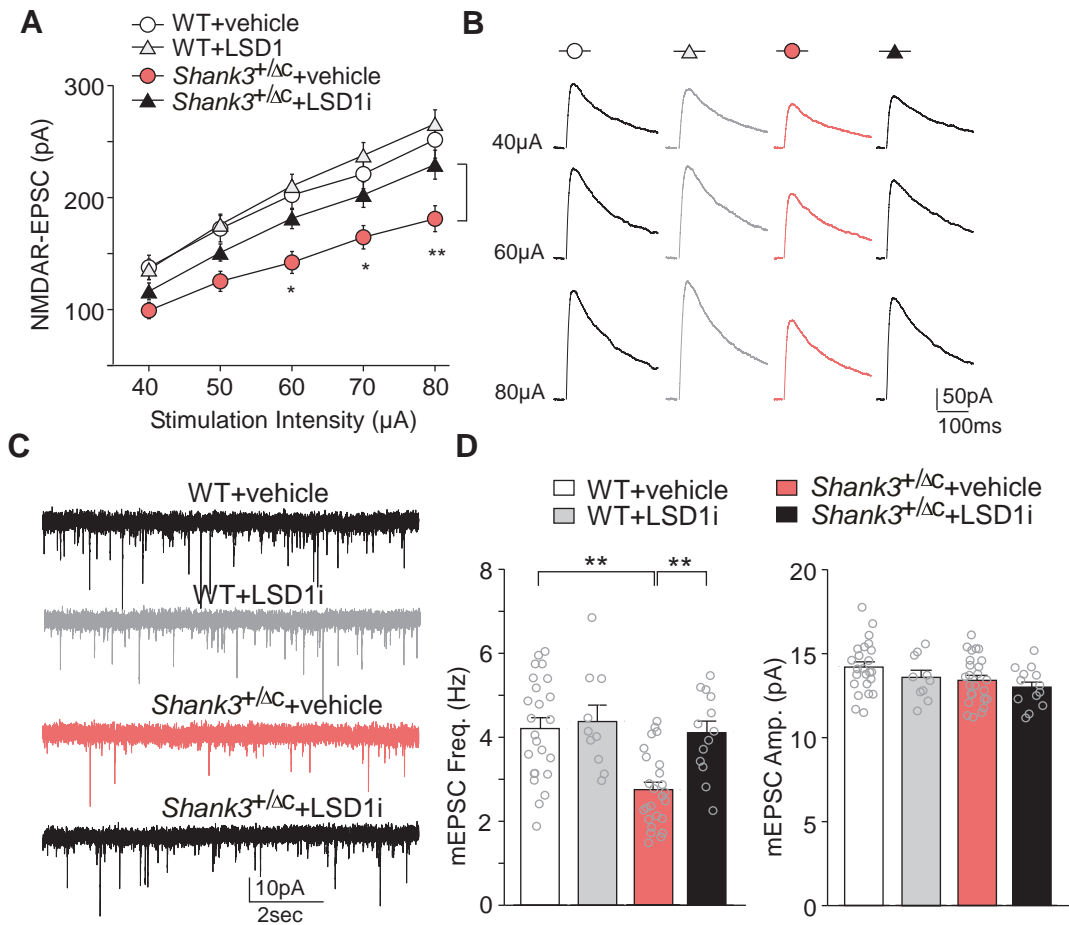


Fig. 4 Treatment of *Shank3*-deficient mice with LSD1 inhibitor rescues NMDAR hypofunction in PFC and restores synaptic response in striatum. **A** Summarized input-output curves of NMDAR-EPSC in PFC pyramidal neurons from WT or *Shank3*^{+/-ΔC} injected with saline or GSK-LSD1 (WT + veh: $n = 9$ cells/3 mice, WT + LSD1i: $n = 11$ cells/3 mice, *Shank3*^{+/-ΔC} + veh: $n = 15$ cells/4 mice, *Shank3*^{+/-ΔC} + LSD1i: $n = 16$ cells/4 mice, $F_{(12,188)}_{\text{group}} = 5.0$, $p < 0.001$; two-way repeated measure ANOVA). **B** Representative NMDAR-EPSC traces. **C** Representative miniature EPSC (mEPSC) traces in striatal medium spiny neurons from WT or *Shank3*^{+/-ΔC} injected with GSK-LSD1 or vehicle. **D** Bar graphs showing mEPSC frequency and amplitude in the four groups (WT + veh: $n = 24$ cells/6 mice, WT + LSD1i: $n = 10$ cells/3 mice, *Shank3*^{+/-ΔC} + veh: $n = 25$ cells/6 mice, *Shank3*^{+/-ΔC} + LSD1i: $n = 13$ cells/4 mice, $F_{(1,68)} = 4.9$, $p = 0.03$; two-way ANOVA). All data are mean \pm SEM. In all figures, * $p < 0.05$, ** $p < 0.01$.

repetitive behaviors, in the *Shank3* model of autism without obvious side effects.

In addition to GSK-LSD1, the therapeutic potential of other LSD1-targeting agents was also examined. ORY-1001, a highly potent and selective clinical stage LSD1 inhibitor ($IC_{50} = 18$ nM, [25]), was used. Systemic administration of ORY-1001 (0.015 mg/kg, i.p., once daily for 3 days) elevated the H3K4me2 level in PFC neurons (Fig. 2F). Behavioral assays indicated that ORY-1001 treatment significantly improved sociability of *Shank3*^{+/-ΔC} mice (Fig. 2G), but not stereotypic grooming (Fig. 2H).

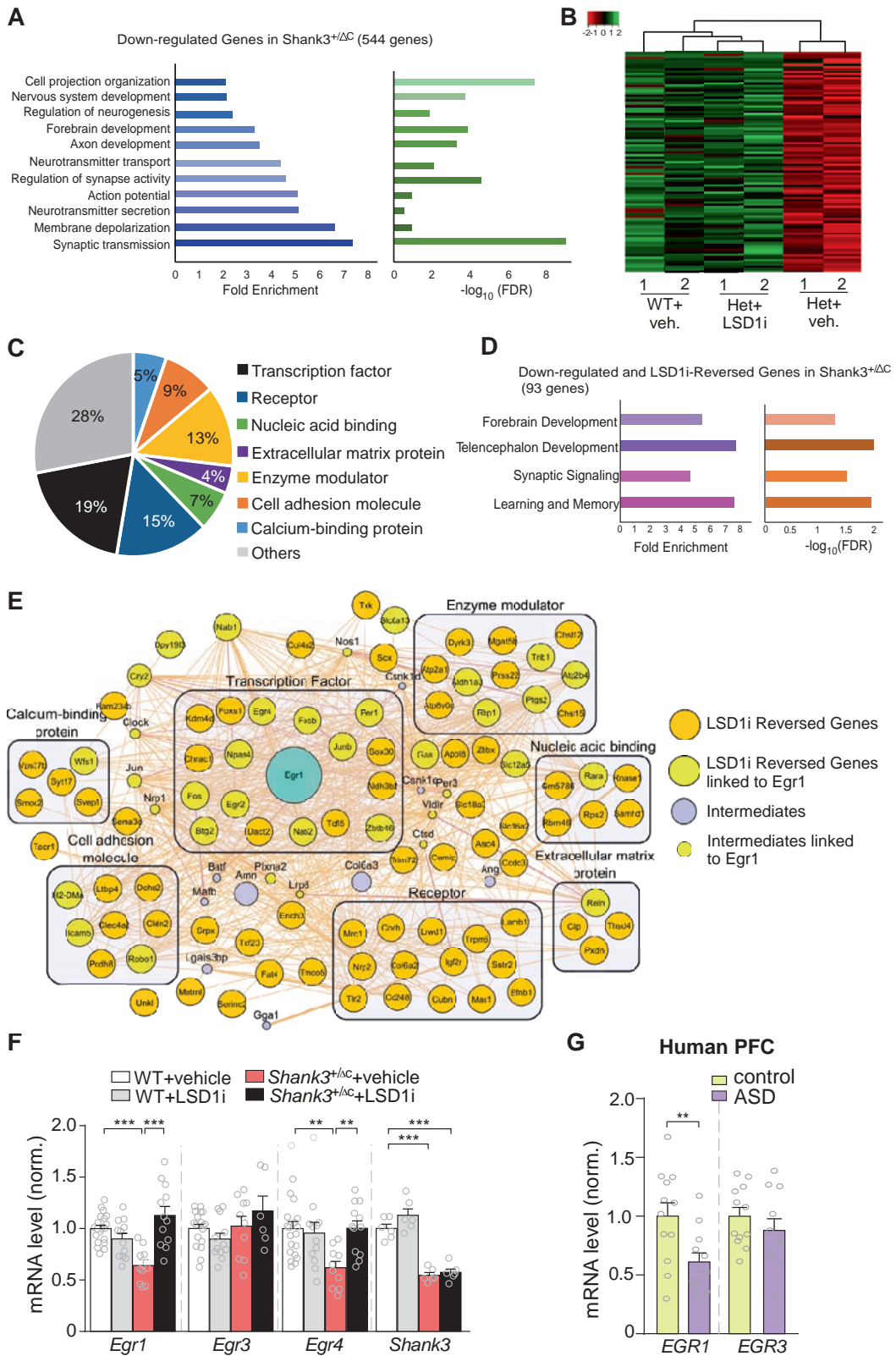
To further determine the significance of our findings in ASD cases associated with *Shank3* deletion/mutations like Phelan-McDermid Syndrome (PMS), we tested the therapeutic potential of LSD1 inhibitor in another *Shank3*-deficient model, *Shank3*^{E13} mice, which have the insertion of a transcriptional stop cassette prior to exon 13 leading to the loss of two *Shank3* higher molecular weight isoforms [14]. Immunoblotting revealed the significantly reduced H3K4me2 level in PFC of *Shank3*^{E13} mice (Fig. 2I), similar to *Shank3*^{+/-ΔC} mice. Behavioral assays found that GSK-LSD1 treatment of heterozygous *Shank3*^{E13} mice significantly improved social preference in the 3-chamber assay (Fig. 2J) and reduced stereotypic grooming (Fig. 2K).

To find out the general applicability, we examined the therapeutic effects of LSD inhibitor in an autism model beyond

Shank3, heterozygous forebrain *Cul3* KO mice (referred as *Cul3*^{f/-}, [26], which carries forebrain deficiency of the top-ranking high-risk autism gene *Cullin 3* (*Cul3*) [1, 27]. *Cul3* encodes a core component of the E3 ubiquitin ligase complex that is responsible for the recognition and recruitment of substrates that needs to be ubiquitinated and degraded [28, 29]. Our recent studies have found that *Cul3*^{f/-} mice exhibit autism-like behavioral deficits, including social preference deficits [26]. Immunostaining showed that PFC neurons from *Cul3*^{f/-} mice exhibited the significantly decreased H3K4me2 signaling, compared to those from *Cul3*^{f/f} control mice (Fig. 3A). Western blotting analyses also revealed the reduced H3K4me2 level in PFC of *Cul3*^{f/-} mice (Fig. 3B). Behavioral studies found that in 3-chamber sociability tests, *Cul3*^{f/-} mice had a significantly lower social preference index than *Cul3*^{f/f} mice, and GSK-LSD1 treatment significantly improved the social preference of *Cul3*^{f/-} mice (Fig. 3C). No difference on the time in center was exhibited in mice with *Cul3* deficiency or GSK-LSD1 treatment in open-field tests (Fig. 3D).

LSD1 inhibitor rescues synaptic function in PFC and striatum of *Shank3*-deficient mice

Since NMDAR hypofunction is a key pathophysiological mechanism for autism [11, 12, 17, 30, 31], we first tested whether the rescue of



NMDARs might underlie the effect of LSD1 inhibitor on social deficits in *Shank3^{+/-ΔC}* mice. Deep layer (L5) frontal cortical pyramidal neurons exhibit the clearest deficits in autistic children [22], so we focused on the electrophysiological recording of these neurons. As shown in Fig. 4A, B, NMDAR-mediated excitatory postsynaptic

currents (EPSC) was significantly diminished in PFC neurons from *Shank3^{+/-ΔC}* mice, consistent with our previous findings [11, 12, 17], and GSK-LSD1 treatment (5 mg/kg, i.p., 3x) elevated NMDAR-EPSC to the control level. It suggests that NMDAR hypofunction in PFC of *Shank3*-deficient mice is rescued by LSD1 inhibition.

Fig. 5 Treatment with LSD1 inhibitor induces genome-wide restoration of down-regulated genes in PFC of *Shank3*-deficient mice. **A** GO biological process (BP) analysis of RNAseq data on down-regulated genes in *Shank3*^{+/ Δ C} mice, compared to WT mice. **B** A heat map representing expression (row z-score) of 93 genes downregulated in *Shank3*^{+/ Δ C} samples (Het) and reversed in GSK-LSD1-treated *Shank3*^{+/ Δ C} samples (LSD1i), compared to wild-type samples (WT). **C, D** Molecular function classification (**C**) and GO BP analysis (**D**) of the 93 down-regulated and LSD1i-restored genes. **E** Interactome network of the 93 down-regulated and LSD1i-restored genes. *Egr1* is identified as a “hub” gene with high connectivity with many other genes. **F** Bar graphs showing the mRNA level of *Egr1*, *Egr3*, *Egr4*, and *Shank3* in WT or *Shank3*^{+/ Δ C} mice without or with GSK-LSD1 treatment ($n = 6\text{--}20$ mice/group, *Egr1*: $F_{(1,50)\text{interaction}} = 27.1$, $p < 0.0001$, *Egr4*: $F_{(1,50)\text{interaction}} = 6.9$, $p = 0.01$, *Shank3*: $F_{(1,20)\text{interaction}} = 1.4$, $p = 0.2$). **G** Bar graphs showing the mRNA level of *EGR1* and *EGR3* in postmortem PFC tissues (BA9) from autism human patients (ASD, $n = 12$) vs. control subjects ($n = 12$) ($t_{22} = 2.8$, $p = 0.01$, t -test). All data are mean \pm SEM. In all figures, * $P < 0.05$, ** $P < 0.01$, *** $P < 0.001$.

To understand the physiological basis that might underlie the effect of LSD1 inhibitor on repetitive behaviors in *Shank3*^{+/ Δ C} mice, we turned to the electrophysiological recording of medium spiny neurons (MSNs) in the striatum, because the altered synaptic signaling in MSNs was found to be associated with the repetitive behaviors in *Shank3*-deficient mice [13, 32]. As shown in Fig. 4C, D, miniature EPSC (mEPSC), a synaptic response resulting from quantal release of single glutamate vesicles, has significantly diminished frequency in MSNs from *Shank3*^{+/ Δ C} mice, and GSK-LSD1 treatment (5 mg/kg, i.p., 3x) elevated mEPSC frequency to the control level. The amplitude of mEPSC was not altered by *Shank3* deficiency or GSK-LSD1 treatment. It suggests that the loss of synaptic inputs in MSNs of *Shank3*-deficient mice is rescued by LSD1 inhibition.

LSD1 inhibitor restores gene expression in PFC of *Shank3*-deficient mice

To find out the molecular basis that may underlie the LSD1 inhibitor-induced rescue of synaptic and behavioral deficits in *Shank3*-deficient mice, we performed the non-biased transcriptomic analysis, RNAseq, to examine the genome-wide effects of GSK-LSD1 on gene expression. PFC of WT vs. *Shank3*^{+/ Δ C} mice without or with GSK-LSD1 treatment (5 mg/kg, i.p., 3x) was collected for mRNA profiling. Compared to WT mice, 544 genes showed the downregulated expression (at least 1.35 fold and $p < 0.05$) in *Shank3*^{+/ Δ C} mice (Supplementary Table 3). Gene Ontology (GO) biological process (BP) analysis indicated that the downregulated genes were significantly enriched in categories related to synaptic function, neuronal function, and development (Fig. 5A).

In *Shank3*^{+/ Δ C} mice treated with GSK-LSD1, 93 out of the total of 544 significantly downregulated genes were significantly elevated (Supplementary Table 4). The heatmap generated with the expression values for these genes (Fig. 5B) show that *Shank3*^{+/ Δ C} samples (Het-a, Het-b) clustered separately from WT samples (WT-a, WT-b), and GSK-LSD1-treated *Shank3*^{+/ Δ C} samples (LSD1-a, LSD1-b) were closer to those from WT samples than *Shank3*^{+/ Δ C} samples. Molecular function classification of the RNAseq data indicated that many of the down-regulated and GSK-LSD1-restored genes fell into the categories including transcription factor, receptor, enzyme modulator, cell adhesion molecule, calcium-binding protein and nucleic acid binding protein (Fig. 5C). GO BP analysis showed that the restored genes were enriched in categories like development, learning, memory, and synaptic signaling (Fig. 5D). Network analysis (Fig. 5E) indicated strong connectivity between transcription factors highly associated with neuronal activity, including *Egr1*, *Egr2*, *Egr4*, *Fos*, *Fosb*, *Junb*, *Npas4*, and *Per1*.

RNAseq also found 698 genes showing upregulated expression (at least 1.35 fold and $p < 0.05$) in *Shank3*^{+/ Δ C} mice (Supplementary Table 5). GO BP analysis indicated that the upregulated genes were enriched in categories related to glial function (Supplementary Fig. S3A). GSK-LSD1 treatment normalized 137 upregulated genes (Supplementary Fig. S3B, Supplementary Table 6), and they were enriched in categories like myelination, oligodendrocyte differentiation, and gliogenesis (Supplementary Fig. S3C).

Molecular function classification and interactome network analysis found that many of the upregulated and GSK-LSD1-normalized genes were enzyme modulators (Supplementary Fig. S3D), which were highly connected (Supplementary Fig. S3E).

To validate the RNAseq results, we performed qPCR to examine the mRNA levels of selected genes. Because of the loss of permissive H3K4me2 in *Shank3*^{+/ Δ C} mice, we particularly focused on the downregulated genes that were rescued by GSK-LSD1. On the top list (>1.5 fold change and $FDR < 0.02$), we identified *Egr1* and *Egr4* genes encoding early growth response proteins, which function as transcription regulatory factors. The induction of these immediate early genes has been tightly linked to neuronal plasticity [33]. We found that the mRNA level of *Egr1* and *Egr4* genes were significantly diminished in PFC of *Shank3*^{+/ Δ C} mice, and GSK-LSD1 treatment dramatically elevated their transcription (Fig. 5F). Other tested genes were either unchanged, such as *Egr3*, or not restored by GSK-LSD1 treatment, such as *Shank3*. Interestingly, a significant loss of *EGR1* mRNA was also found in postmortem PFC (BA9) from idiopathic autism human patients, compared to control subjects (Fig. 5G). It suggests that *Egr1* may play an important role in ASD pathophysiology.

Egr1 is a key molecular target of LSD1 involved in social behavior

RNAseq has identified *Egr1* as a top-ranking downregulated gene rescued by GSK-LSD1 treatment. To find out whether the alteration of *Egr1* transcription is due to the change in H3K4me2 at *Egr1*, we examined the ChIPseq data to compare H3K4me2 occupancy at *Egr1* promoter and enhancer regions in WT vs. *Shank3*^{+/ Δ C} mice treated with GSK-LSD1. As illustrated in the landscapes (Fig. 6A), at an *Egr1* enhancer region, which is occupied by LSD1 as shown in the genome browser snapshots [34] presenting the coinciding relevant loci, H3K4me2 enrichment was significantly decreased in *Shank3*^{+/ Δ C} mice and was restored by GSK-LSD1 treatment. It suggests that LSD1-mediated regulation of H3K4me2 directly contributes to *Egr1* transcriptional changes.

To find out whether *Egr1* is a key molecular target of LSD1 involved in autism, we examined the effect of *Egr1* overexpression in PFC of *Shank3*^{+/ Δ C} mice on autistic behavioral deficits. As shown in Figs. 6B, C, stereotaxic injection of *Egr1* AAV to medial PFC significantly increased the expression level of *Egr1* in *Shank3*^{+/ Δ C} mice. Behavioral assays found that *Egr1*-injected *Shank3*^{+/ Δ C} mice had significantly improved social interaction time and social preference index in 3-chamber sociability tests (Fig. 6D). However, *Egr1* overexpression in PFC of *Shank3*^{+/ Δ C} mice failed to mitigate stereotypic grooming (Fig. 6E). Locomotion or anxiety was unaltered in *Egr1*-injected *Shank3*^{+/ Δ C} mice (Fig. 6F, G). These data suggest that *Egr1* in PFC plays a critical role in regulating sociability.

LSD1 inhibition improves H3K4me2 occupancy genome-wide and in genes related to ASD and development

Given the reduction of H3K4me2 in *Shank3*^{+/ Δ C} mice and the restoration of gene expression by LSD1 inhibition, we further performed ChIP-seq to examine the genome-wide alteration of

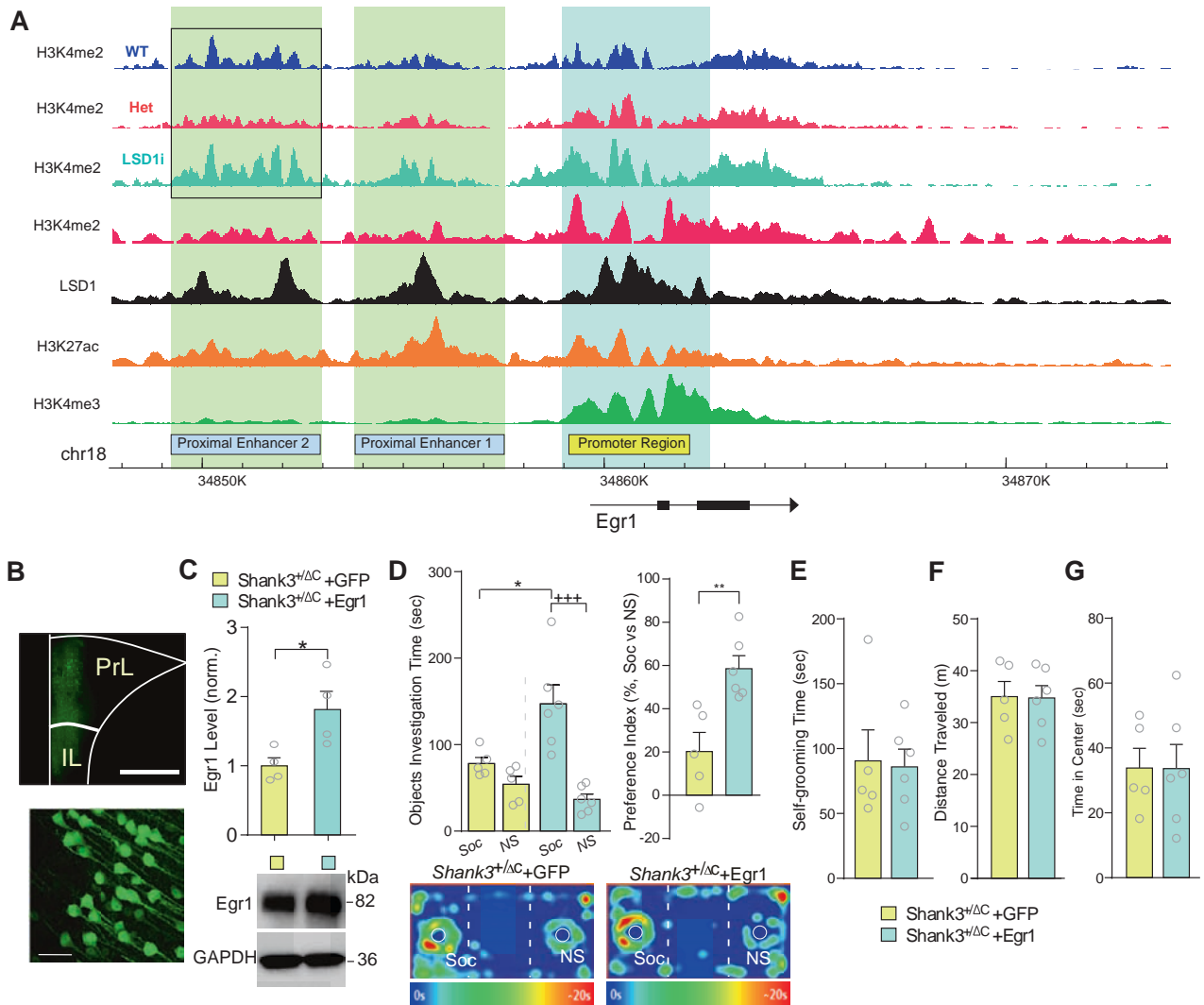


Fig. 6 Overexpression of Egr1 in PFC of *Shank3*-deficient mice rescues autism-like social deficits. **A** ChIP-seq data showing H3K4me2 enrichment at *Egr1* enhancer and promoter regions in wild-type (WT), *Shank3*^{+/ Δ C} mice (Het) or *Shank3*^{+/ Δ C} treated with GSK-LSD1 (LSD1i). Boxed area highlights the *Egr1* enhancer region with changed H3K4me2 peaks, which coincides with LSD1 occupancy at the same locus [34]. Promoter and enhancer regions are identified by the occupancy loci of histone marks H3K4me2, H3K27ac, and H3K4me3 [34]. **B** Images showing the viral expression in prelimbic (PrL) and infralimbic (IL) neurons. Scale bars: 1000 μ m (low magnification) and 40 μ m (high magnification). **C** Bar graphs and representative blots showing the level of Egr1 in PFC from *Shank3*^{+/ Δ C} mice injected with Egr1 AAV or GFP AAV ($n = 4$ /group, $t_6 = 2.8$, $p = 0.03$; t -test). **D** Bar graphs showing the investigation time and social preference index in the 3-chamber sociability testing of *Shank3*^{+/ Δ C} mice with PFC injection of Egr1 AAV ($n = 6$) or GFP AAV ($n = 5$) (time: $F_{(1,18)interaction} = 9.8$, $p = 0.006$. two-way ANOVA; index: $t_9 = 3.7$, $p = 0.005$, t -test). Inset: Representative heat maps of the sociability tests. **E-G** Bar graphs showing the time on self-grooming (**E**), locomotor activity (**F**), and time in center of open-field test (**G**) in *Shank3*^{+/ Δ C} mice with PFC injection of Egr1 AAV ($n = 6$) or GFP AAV ($n = 5$). All data are mean \pm SEM. In all figures, * $p < 0.05$, ** $p < 0.01$, *Shank3*^{+/ Δ C} + GFP vs. *Shank3*^{+/ Δ C} + Egr1; +++ $p < 0.01$, Soc vs. NS.

H3K4me2 occupancy in *Shank3*^{+/ Δ C} mice and the effects of GSK-LSD1 treatment. PFC neuronal nuclei was sorted by flow cytometry as previously described [35]. Compared to WT mice, genome-wide occupancy of H3K4me2 around the transcription start site (TSS) was reduced in PFC neurons from *Shank3*^{+/ Δ C} mice, which was partially reversed in GSK-LSD1-treated mice (Fig. 7A). The genes with the diminished H3K4me2 occupancy ($p < 0.01$, *Shank3*^{+/ Δ C} vs. WT) but reversed by GSK-LSD1 treatment ($p < 0.05$, *Shank3*^{+/ Δ C} + LSD1i vs. *Shank3*^{+/ Δ C}) (Supplementary Table 7) were enriched in categories like regulation of signaling, neural development, and transcription (Fig. 7B, top). The H3K4me2 landscapes at the promoter region of selected genes in the enriched pathways are shown in Supplementary Fig. S4. The genes with both reduced H3K4me2 occupancy ($p < 0.01$, *Shank3*^{+/ Δ C} vs. WT) and decreased mRNA expression (FC > 1.35, $p < 0.05$,

Shank3^{+/ Δ C} vs. WT) (Supplementary Table 8) were enriched in synaptic function and neural development (Fig. 7B, bottom). The genes with GSK-LSD1 reversal of both H3K4me2 occupancy and mRNA expression (Supplementary Table 9) included *Syt17* (Synaptotagmin-17), a brain-specific molecule controlling synaptic exocytosis and neurotransmitter release, *Slc16a2* (Solute Carrier), a transporter of thyroid hormone that plays a critical role in nervous system development, and *Reln* (Reelin), an ASD-associated molecule regulating neuronal migration and brain plasticity.

Gene set enrichment analysis (GSEA) revealed that the genes with reduced H3K4me2 occupancy in *Shank3*^{+/ Δ C} mice were significantly correlated with the ASD genes altered in PFC/ACC of ASD patients [36] and the SFARI ASD risk gene set (Fig. 7C). Treatment of *Shank3*^{+/ Δ C} mice with GSK-LSD1 effectively restored the level of H3K4me2 enrichment in selected genes from

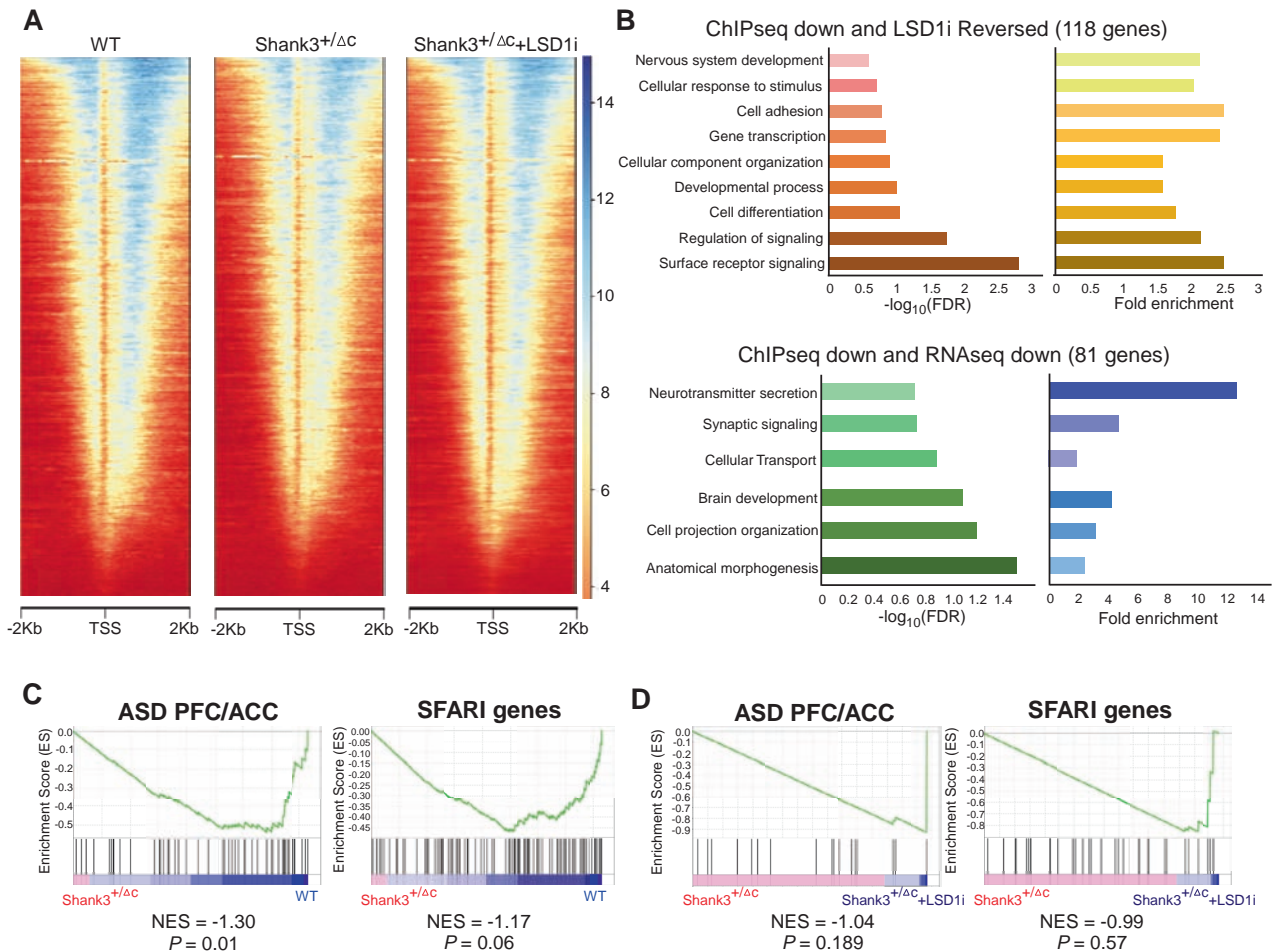


Fig. 7 Treatment with LSD1 inhibitor induces genome-wide restoration of H3K4me2 occupancy at gene promoters in PFC of *Shank3*-deficient mice. **A** Heat maps showing global H3K4me2 occupancy at the gene promoter region (± 2 kb around TSS) in PFC neurons from WT, *Shank3*^{+/ Δ C}, and *Shank3*^{+/ Δ C} + LSD1i mice. LSD1i: GSK-LSD1. Note the difference on blue signals (darker blue for higher H3K4me2 enrichment). **B** GO analysis of the genes with a significant reduction of H3K4me2 occupancy and reversed by LSD1i treatment in *Shank3*^{+/ Δ C} mice (top), and GO analysis of the genes with a significant reduction of both H3K4me2 occupancy and mRNA expression in *Shank3*^{+/ Δ C} mice (bottom). **C**, **D** GSEA analysis of the correlation between genes with significantly lower H3K4me2 occupancy (C: *Shank3*^{+/ Δ C} vs. WT; D: *Shank3*^{+/ Δ C} vs. *Shank3*^{+/ Δ C} + LSD1i) and the altered genes in PFC/ACC (anterior cingulate cortex) regions from ASD patients or SFARI risk gene set.

both of these datasets (Fig. 7D). These data further support that GSK-LSD1 is an effective treatment in recovering H3K4me2-mediated transcription of ASD risk genes in *Shank3*^{+/ Δ C} mice.

DISCUSSION

In this study, we have revealed the aberration of H3K4me2 in PFC of mouse models with the deficiency of distinct autism risk factors – *Shank3* and *Cul3*. The diminished H3K4me2 is recapitulated in PFC of idiopathic autistic human patients, suggesting that this epigenetic alteration is a conserved abnormality in ASD. While H3K4me2 is reduced in the prefrontal cortex of ASD, no significant change in the level of H3K4me2 is found in the striatum of *Shank3*^{+/ Δ C} mice. The exact reason for the region specificity of this histone mark in ASD is unclear, however, many studies have reported epigenetic alterations and therapeutic interventions in a region-specific manner [11, 37, 38]. Given the profound differences between PFC pyramidal neurons and striatal medium spiny neurons, it is not surprising that they have distinct epigenetic profiles.

Inhibiting LSD1 to normalize H3K4me2 provides significant amelioration of two core symptoms of ASD, social impairments and stereotypic behaviors, in two different *Shank3*-deficient mouse

models (*Shank3*^{+/ Δ C} and *Shank3*^{E13}). In addition, LSD1 inhibitor rescues social deficits in forebrain *Cul3* KO mice, suggesting the general applicability of this intervention. Interestingly, antagonizing LSD1 activity also reverses schizophrenia-related cognitive and morphological phenotypes in *Setd1a*-deficient mice [34].

Electrophysiological data reveals the potential basis for the amelioration of behavioral deficits by LSD1 inhibitors. We have previously shown that the specifically diminished NMDAR function in the PFC of *Shank3*^{+/ Δ C} mice and forebrain *Cul3* knockout (*Cul3*^{f/f}) mice is strongly linked to social preference impairment [11, 12, 17, 26, 39–41]. The restoration of NMDAR-mediated synaptic response in PFC neurons by inhibiting LSD1 may underlie the therapeutic effects of LSD1 inhibitors on social deficits in these ASD models.

The therapeutic effect of GSK-LSD1 on repetitive grooming may be attributable to the rescue of the diminished synaptic signaling in striatum of *Shank3*^{+/ Δ C} mice, a brain region critical for stereotypic behaviors [42]. Despite the link of striatal dysfunction to the increased grooming behavior, it is the stimulation of corticostriatal circuit (orbitofrontal cortex to ventromedial striatum) that is required for inducing increased grooming [43]. Corticostriatal circuit abnormalities are suggested to underlie ASD-like behaviors, such as increased grooming, in *Shank3*-deficient

mice [13, 15]. Excessive grooming in an OCD model (Sapap3-knockout mice) is also found to be associated with synaptic deficits in the specific corticostriatal projections (motor and cingulate cortex to dorsolateral and dorsomedial striatum) [44]. GSK-LSD1 restores striatal synaptic responses to glutamatergic inputs from the cortex and reduces grooming behavior, which could be due to its elevation of H3K4me2 level in PFC neurons and the ensuing restoration of PFC control of striatal activity. Future studies will examine synaptic mechanisms underlying the altered mEPSC frequency in striatal medium spiny neurons, including changes in excitatory synapse numbers, presynaptic release from cortical inputs, or postsynaptic receptors and signaling molecules.

One important feature of the therapeutic effects of LSD1 inhibitor GSK-LSD1 is its effectiveness on two core autism-related phenotypes, social deficits, and repetitive grooming. Most of the epigenetic drugs we tested, including inhibitors for class I HDACs [11, 39], EHMT1/2 [17] and Smyd3 [26], have only ameliorated social impairment. However, another LSD1 inhibitor ORY-1001 only rescued social defect, but not repetitive behaviors. The reason for this difference may be related to the different structures and pharmacological profiles (e.g. potency, selectivity, brain permeability, pharmacokinetics and pharmacodynamics) of these two compounds [25]. More detailed studies on ORY-1001 will help to clarify it.

Another important feature of the therapeutic effects of GSK-LSD1 is the long duration. After a 3-day treatment, social improvement lasted for ~8 days, and repetitive behavior improvement lasted for ~21 days. Although a significant increase of H3K4me3 in PFC is only found on day 1 after treatment cessation, this increase may provide a trigger to induce gene transcriptional changes, which leads to long-lasting behavioral alterations, similar to the long-lasting effects of other epigenetic drugs [11, 17, 39]. Since social and self-grooming are totally different behaviors, their different sensitivities to neural changes in distinct brain circuits may underlie the different temporal profiles of the rescue effects of GSK-LSD1. Detailed temporal and spatial profiling of the pharmacological treatment with LSD1 inhibitors on various *in vitro* readouts will be pursued in follow-up studies.

RNA-seq data have identified potential molecular basis for the rescue of behavioral and physiological deficits in Shank3-deficient mice by targeting LSD1. Distinct up- and down-regulated genes in PFC of Shank3^{+/ Δ C} mice suggest that a complex set of genes collectively contributes to the phenotypes. Particularly interesting genes are the down-regulated ones reversed by LSD1 inhibition, which are enriched in synaptic signaling and development. Among them, Egr1 is identified as the top-ranking “hub” gene.

Egr1 (early growth response 1), the immediate early gene and transcription factor, is a major controller of synaptic plasticity and neuronal activity in physiological conditions and neuropsychiatric disorders [33, 45]. Egr1 is regulated by various environmental stimuli, such as social experiences, stress, and learning tasks, and can trigger neuronal activity changes, growth factor release, or hormone secretion. In mouse cortex, Egr1 binds to the close vicinity of TSS of a number of genes enriched in biological pathways related to cell-cell recognition and communication [33, 46], therefore exerts a large transcriptional control on critical processes underlying synaptic plasticity and encoding of information. There have been reports that Egr1 is downregulated in PFC of human patients suffering from major depression [47] or schizophrenia [48, 49]. Here we find that Egr1 is significantly diminished in PFC of ASD humans and Shank3-deficient mice, which is restored by LSD1 inhibitor.

The alteration of H3K4me2 occupancy at Egr1 promoter by Shank3 deficiency and LSD1 inhibition is well correlated with Egr1 transcriptional changes, suggesting that Egr1 is epigenetically

regulated by LSD1. In agreement with this, LSD1 regulates the chromatin state of Egr1 by interacting with transcription factor serum response factor (SRF) in mouse hippocampus [50]. Overexpressing Egr1 in PFC of Shank3-deficient mice restores social preference, pointing to Egr1 as a potential new target for autism treatment. A growing body of evidence also relates the expression levels of Egr1 with sociability [51–53]. Molecular mechanisms underlying the effect of Egr1 overexpression on social behaviors awaits to be further studied.

ChIP-seq data have revealed the genome-wide alterations of H3K4me2 occupancy at gene promoters by Shank3 deficiency and LSD1 inhibition. Genes with the diminished H3K4me2 occupancy but reversed by GSK-LSD1 treatment are enriched in neural signaling and development, consistent with RNAseq data. These genes are highly correlated with ASD risk factors found in human samples, emphasizing the translational values of our preclinical studies.

In summary, this preclinical study has revealed a new connection between epigenetic aberration and ASD pathophysiology. Results from our multilevel interrogations suggest that targeting the histone demethylase and transcriptional corepressor LSD1 or the key downstream molecular target Egr1 provides a promising avenue for treating core symptoms of ASD.

EXPERIMENTAL PROCEDURES

Animals and human postmortem tissue

Shank3^{+/ Δ C}, Shank3^{E13}, Cul3^{ff}, and Cul3^{fl} mice were bred, genotyped, and maintained as previously described [11, 12, 14, 26]. Animals were group-housed with food and water *ad libitum* in controlled temperature (22–23 °C) and humidity conditions and kept under a 12/12 h light/dark cycle. Mice were 4 weeks old at the time of surgery. Behavioral testing, electrophysiological recording, or tissue harvesting were performed at the age of 6 weeks old. Only male Shank3^{+/ Δ C} mice were used because of normal sociability in female Shank3^{+/ Δ C} mice [11, 12, 24]. Both sexes of other lines of animals were used. All experimental procedures followed protocols approved by the University at Buffalo Institutional Animal Care and Use Committee. Postmortem brain tissue samples (Broadman's area 9) were received from NIH NeuroBioBank.

Drug administration and viral injection

GSK-LSD1 (Tocris, Cat. # 5361) or ORY-1001 (SelleckChem, CAS # 1431326-61-2) was dissolved in water as a stock solution and then further diluted in sterile saline as working solution. Mice were injected with GSK-LSD1 (5 mg/kg, *i.p.*), ORY-1001 (0.015 mg/kg, *i.p.*) or vehicle control once daily for three consecutive days.

For viral injection, the mouse was deeply anesthetized with ketamine/xylazine (100 mg/kg; 10 mg/kg) and placed in a stereotaxic frame (Stoelting, USA). Under standard and sterile surgical conditions, a 10 μ l syringe (7000 series, Hamilton, USA) attached to a micropump was lowered through to skull burr hole into the PFC (AP + 1.8 mm, L \pm 0.3 mm, DV –2.7 mm). Mice were injected with either AAV2-CMV-GFP or AAV2-CMV-EGR1-Flag in the PFC (0.3 μ l per hemisphere) at a flow rate of 50 nl/min.

Behavioral procedures

Mice performing behavioral tasks were traced and recorded by ANY-maze (Stoelting, USA) for quantification analyses [11, 12, 26]. Mice of different genotypes were randomly assigned to treatment groups and tested blindly. See Supplementary Methods for details regarding Social Preference Test, Stereotypic Behavior, Rotorod, Locomotion, and Open-field tests.

Electrophysiological recordings

See Supplementary Methods for details regarding patch-clamp recordings in slices.

Immunofluorescence and confocal imaging

See Supplementary Methods for details.

Immunoblotting

See Supplementary Methods for details.

RNA-seq and bioinformatics analysis

See Supplementary Methods for details.

Quantitative PCR

See Supplementary Methods for details.

H3K4me2 ChIP-seq with neuronal nuclei and data analysis

See Supplementary Methods for details.

Statistics

All data were expressed as the mean \pm SEM. All groups were tested for normality via Shapiro-Wilks tests. No sample was excluded from the analysis. The sample size was based on power analyses and was similar to those reported in previous works. The variance between groups being statistically compared was similar. Each set of the experiments was replicated for at least three times. Experiments with two groups were compared using Student's *t*-tests. Experiments with more than two groups were subjected to one-way ANOVA, two-way ANOVA, or two-way repeated measure ANOVA, followed by *post hoc* Bonferroni tests.

DATA AVAILABILITY

The RNAseq and ChIPseq data generated in this study have been deposited in the GEO public repository under accession code GSE193380.

REFERENCES

- De Rubeis S, He X, Goldberg AP, Poultney CS, Samocha K, Cicek AE, et al. Synaptic, transcriptional and chromatin genes disrupted in autism. *Nature*. 2014;515:209–15.
- Coe BP, Stessman HAF, Sulovari A, Geisheker MR, Bakken TE, Lake AM, et al. Neurodevelopmental disease genes implicated by de novo mutation and copy number variation morbidity. *Nat Genet*. 2019;51:106–16.
- Stessman HA, Xiong B, Coe BP, Wang T, Hoekzema K, Fencckova M, et al. Targeted sequencing identifies 91 neurodevelopmental-disorder risk genes with autism and developmental-disability biases. *Nat Genet*. 2017;49:515–26.
- Geschwind DH, State MW. Gene hunting in autism spectrum disorder: on the path to precision medicine. *Lancet Neurol*. 2015;14:1109–20.
- Jambhekar A, Dhall A, Shi Y. Roles and regulation of histone methylation in animal development. *Nat Rev Mol Cell Biol*. 2019;20:625–41.
- Tunovic S, Barkovich J, Sherr EH, Slavotinek AM. De novo ANKRD11 and KDM1A gene mutations in a male with features of KBG syndrome and Kabuki syndrome. *Am J Med Genet A*. 2014;164A:1744–9.
- Shen E, Shulha H, Weng Z, Akbarian S. Regulation of histone H3K4 methylation in brain development and disease. *Philos Trans R Soc Biol Sci* 2014;369:20130514.
- Shulha HP, Cheung I, Whittle C, Wang J, Virgil D, Lin CL, et al. Epigenetic signatures of autism: trimethylated H3K4 landscapes in prefrontal neurons. *Arch Gen Psychiatry*. 2012;69:314–24.
- Betancur C, Buxbaum JD. SHANK3 haploinsufficiency: a “common” but underdiagnosed highly penetrant monogenic cause of autism spectrum disorders. *Mol Autism*. 2013;4:17.
- Leblond CS, Nava C, Polge A, Gauthier J, Huguet G, Lumbroso S, et al. Meta-analysis of SHANK mutations in autism spectrum disorders: a gradient of severity in cognitive impairments. *PLoS Genet*. 2014;10:e1004580.
- Qin L, Ma K, Wang ZJ, Hu Z, Matas E, Wei J, et al. Social deficits in Shank3-deficient mouse models of autism are rescued by histone deacetylase (HDAC) inhibition. *Nat Neurosci*. 2018;21:564–75.
- Duffney LJ, Zhong P, Wei J, Matas E, Cheng J, Qin L, et al. Autism-like deficits in Shank3-Deficient mice are rescued by targeting actin regulators. *Cell Rep*. 2015;11:1400–13.
- Peca J, Feliciano C, Ting JT, Wang W, Wells MF, Venkatraman TN, et al. Shank3 mutant mice display autistic-like behaviours and striatal dysfunction. *Nature*. 2011;472:437–42.

- Jaramillo TC, Speed HE, Xuan Z, Reimers JM, Escamilla CO, Weaver TP, et al. Novel Shank3 mutant exhibits behaviors with face validity for autism and altered striatal and hippocampal function. *Autism Res*. 2017;10:42–65.
- Wang X, Bey AL, Katz BM, Badea A, Kim N, David LK, et al. Altered mGluR5-Homer scaffolds and corticostriatal connectivity in a Shank3 complete knockout model of autism. *Nat Commun*. 2016;7:11459.
- Wang X, McCoy PA, Rodriguiz RM, Pan Y, Je HS, Roberts AC, et al. Synaptic dysfunction and abnormal behaviors in mice lacking major isoforms of Shank3. *Hum Mol Genet*. 2011;20:3093–108.
- Wang ZJ, Zhong P, Ma K, Seo JS, Yang F, Hu Z, et al. Amelioration of autism-like social deficits by targeting histone methyltransferases EHMT1/2 in Shank3-deficient mice. *Mol Psychiatry*. 2020;25:2517–33.
- Lee MG, Wynder C, Bochar DA, Hakimi MA, Cooch N, Shiekhhattar R. Functional interplay between histone demethylase and deacetylase enzymes. *Mol Cell Biol*. 2006;26:6395–402.
- Nair SS, Li DQ, Kumar R. A core chromatin remodeling factor instructs global chromatin signaling through multivalent reading of nucleosome codes. *Mol Cell*. 2013;49:704–18.
- Meier K, Brehm A. Chromatin regulation: how complex does it get? *Epigenetics*. 2014;9:1485–95.
- Yan Z, Rein B. Mechanisms of synaptic transmission dysregulation in the prefrontal cortex: pathophysiological implications. *Mol Psychiatry*. 2021. <https://doi.org/10.1038/s41380-021-01092-3>. Online ahead of print.
- Stoner R, Chow ML, Boyle MP, Sunkin SM, Mouton PR, Roy S, et al. Patches of disorganization in the neocortex of children with autism. *N. Engl J Med*. 2014;370:1209–19.
- Cusan M, Cai SF, Mohammad HP, Krivtsov A, Chramiec A, Loizou E, et al. LSD1 inhibition exerts its antileukemic effect by recommissioning PU.1- and C/EBPalpha-dependent enhancers in AML. *Blood*. 2018;131:1730–42.
- Rein B, Ma K, Yan Z. A standardized social preference protocol for measuring social deficits in mouse models of autism. *Nat Protoc*. 2020;15:3464–77.
- Maes T, Mascaro C, Tirapu I, Estiarte A, Ciceri F, Lunardi S, et al. ORY-1001, a potent and selective covalent KDM1A inhibitor, for the treatment of acute leukemia. *Cancer Cell*. 2018;33:495–511.
- Rapanelli M, Tan T, Wang W, Wang X, Wang ZJ, Zhong P, et al. Behavioral, circuitry, and molecular aberrations by region-specific deficiency of the high-risk autism gene Cul3. *Mol Psychiatry*. 2021;26:1491–504.
- O’Roak BJ, Vives L, Girirajan S, Karakoc E, Krumm N, Coe BP, et al. Sporadic autism exomes reveal a highly interconnected protein network of de novo mutations. *Nature*. 2012;485:246–50.
- Chen Y, Yang Z, Meng M, Zhao Y, Dong N, Yan H, et al. Cullin mediates degradation of RhoA through evolutionarily conserved BTB adaptors to control actin cytoskeleton structure and cell movement. *Mol Cell*. 2009;35:841–55.
- Genschik P, Sumara I, Lechner E. The emerging family of CULLIN3-RING ubiquitin ligases (CRL3s): cellular functions and disease implications. *EMBO J*. 2013;32:2307–20.
- Won H, Lee HR, Gee HY, Mah W, Kim JI, Lee J, et al. Autistic-like social behaviour in Shank2-mutant mice improved by restoring NMDA receptor function. *Nature*. 2012;486:261–5.
- Speed HE, Kouser M, Xuan Z, Reimers JM, Ochoa CF, Gupta N, et al. Autism-associated insertion mutation (InsG) of Shank3 exon 21 causes impaired synaptic transmission and behavioral deficits. *J Neurosci*. 2015;35:9648–65.
- Wang W, Li C, Chen Q, van der Goes MS, Hawrot J, Yao AY, et al. Striatopallidal dysfunction underlies repetitive behavior in Shank3-deficient model of autism. *J Clin Invest*. 2017;127:1978–90.
- Duclot F, Kabbaj M. The role of early growth response 1 (EGR1) in brain plasticity and neuropsychiatric disorders. *Front Behav Neurosci*. 2017;11:35.
- Mukai J, Cannavo E, Crabtree GW, Sun Z, Diamantopoulou A, Thakur P, et al. Recapitulation and reversal of schizophrenia-related phenotypes in Setd1a-deficient mice. *Neuron*. 2019;104:471–87.
- Kundakovic M, Jiang Y, Kavanagh DH, Dincer A, Brown L, Pothula V, et al. Practical guidelines for high-resolution epigenomic profiling of nucleosomal histones in postmortem human brain tissue. *Biol Psychiatry*. 2017;81:162–70.
- Velmeshev D, Schirmer L, Jung D, Haeussler M, Perez Y, Mayer S, et al. Single-cell genomics identifies cell type-specific molecular changes in autism. *Science*. 2019;364:685–9.
- Maze I, Covington HE 3rd, Dietz DM, LaPlant Q, Renthal W, Russo SJ, et al. Essential role of the histone methyltransferase G9a in cocaine-induced plasticity. *Science*. 2010;327:213–6.
- Hamilton PJ, Burek DJ, Lombroso SI, Neve RL, Robison AJ, Nestler EJ, et al. Cell-type-specific epigenetic editing at the fosb gene controls susceptibility to social defeat stress. *Neuropsychopharmacology*. 2018;43:272–84.
- Ma K, Qin L, Matas E, Duffney LJ, Liu A, Yan Z. Histone deacetylase inhibitor MS-275 restores social and synaptic function in a Shank3-deficient mouse model of autism. *Neuropsychopharmacology*. 2018;43:1779–88.

40. Qin L, Ma K, Yan Z. Chemogenetic activation of prefrontal cortex in Shank3-deficient mice ameliorates social deficits, NMDAR hypofunction, and Sgk2 downregulation. *iScience*. 2019;17:24–35.
41. Qin L, Ma K, Yan Z. Rescue of histone hypoacetylation and social deficits by ketogenic diet in a Shank3 mouse model of autism. *Neuropsychopharmacology*. 2021. <https://doi.org/10.1038/s41386-021-01212-1>. Online ahead of print.
42. Graybiel AM. Habits, rituals, and the evaluative brain. *Annu Rev Neurosci*. 2008;31:359–87.
43. Ahmari SE, Spellman T, Douglass NL, Kheirbek MA, Simpson HB, Deisseroth K, et al. Repeated cortico-striatal stimulation generates persistent OCD-like behavior. *Science*. 2013;340:1234–9.
44. Hadjas LC, Schartner MM, Cand J, Creed MC, Pascoli V, Lüscher C, et al. Projection-specific deficits in synaptic transmission in adult Sapap3-knockout mice. *Neuropsychopharmacology*. 2020;45:2020–9.
45. Knapska E, Kaczmarek L. A gene for neuronal plasticity in the mammalian brain: Zif268/Egr-1/NGFI-A/Krox-24/TIS8/ZENK? *Prog Neurobiol*. 2004;74:183–211.
46. Koldamova R, Schug J, Lefterova M, Cronican AA, Fitz NF, Davenport FA, et al. Genome-wide approaches reveal EGR1-controlled regulatory networks associated with neurodegeneration. *Neurobiol Dis*. 2014;63:107–14.
47. Covington HE 3rd, Lobo MK, Maze I, Vialou V, Hyman JM, Zaman S, et al. Anti-depressant effect of optogenetic stimulation of the medial prefrontal cortex. *J Neurosci*. 2010;30:16082–90.
48. Kimoto S, Bazmi HH, Lewis DA. Lower expression of glutamic acid decarboxylase 67 in the prefrontal cortex in schizophrenia: contribution of altered regulation by Zif268. *Am J Psychiatry*. 2014;171:969–78.
49. Yamada K, Gerber DJ, Iwayama Y, Ohnishi T, Ohba H, Toyota T, et al. Genetic analysis of the calcineurin pathway identifies members of the EGR gene family, specifically EGR3, as potential susceptibility candidates in schizophrenia. *Proc Natl Acad Sci*. 2007;104:2815–20.
50. Rusconi F, Grillo B, Ponzoni L, Bassani S, Toffolo E, Paganini L, et al. LSD1 modulates stress-evoked transcription of immediate early genes and emotional behavior. *Proc Natl Acad Sci*. 2016;113:3651–6.
51. Dossat AM, Jourdi H, Wright KN, Strong CE, Sarkar A, Kabbaj M. Viral-mediated Zif268 expression in the prefrontal cortex protects against gonadectomy-induced working memory, long-term memory, and social interaction deficits in male rats. *Neuroscience*. 2017;340:243–57.
52. Stack A, Carrier N, Dietz D, Hollis F, Sorenson J, Kabbaj M. Sex differences in social interaction in rats: role of the immediate-early gene zif268. *Neuropsychopharmacology*. 2010;35:570–80.
53. Yang Y, Shu X, Liu D, Shang Y, Wu Y, Pei L, et al. EPAC null mutation impairs learning and social interactions via aberrant regulation of miR-124 and Zif268 translation. *Neuron*. 2012;73:774–88.

ACKNOWLEDGEMENTS

We thank Dr. Craig Powell at University of Alabama at Birmingham for kindly providing breeding pairs of Shank3^{E13} mice. We thank Dr. Mohamed Kabbaj at Florida State University for kindly providing Egr1 AAV and GFP AAV. We also thank Xiaoqing Chen for excellent technical support and Luciana R. Frick for taking some confocal images. This work was supported by: Nancy Lurie Marks Family Foundation (ZY), National Institutes of Health (MH112237, MH126443) (ZY), National Center for Advancing Translational Sciences of the National Institutes of Health (KL2TR001413) (MR), and National Institutes of Health (MH104341, MH117790) (SA).

AUTHOR CONTRIBUTIONS

MR performed some behavioral, immunocytochemical, biochemical experiments, bioinformatic analyses, and wrote the draft. JW and FY performed bioinformatic analyses. KM performed behavioral experiments. PZ carried out electrophysiological experiments. RP and MK performed some behavioral and biochemical assays. LQ, BR, Z-JW carried out qPCR or immunocytochemical experiments. BK, BJ, and LC extracted neuronal nuclei for ChIPseq experiments. SA oversaw ChIPseq studies. ZY designed experiments, supervised the project and wrote the paper. None of the authors have the financial interest related to this work.

COMPETING INTERESTS

The authors declare no competing interests.

ADDITIONAL INFORMATION

Supplementary information The online version contains supplementary material available at <https://doi.org/10.1038/s41380-022-01508-8>.

Correspondence and requests for materials should be addressed to Zhen Yan.

Reprints and permission information is available at <http://www.nature.com/reprints>

Publisher's note Springer Nature remains neutral with regard to jurisdictional claims in published maps and institutional affiliations.